Effect of Coulomb correlation on electron transport through a concentric quantum ring–quantum dot structure

T. Chwiej* and K. Kutorasiński
Faculty of Physics and Applied Computer Science, AGH University of Science and Technology, al. Mickiewicza 30, 30-059 Kraków, Poland

(Received 31 July 2009; revised manuscript received 2 February 2010; published 29 April 2010)

We study transfer of a single-electron through a quantum ring capacitively coupled to the charged quantum dot placed in its center. For this purpose we solve the time-dependent Schrödinger equation for the pair of particles: the electron traveling through the ring and the other carrier confined within the quantum dot. The correlation effects due to the interaction between the charge carriers are described in a numerically exact manner. We find that the amplitude of Aharonov-Bohm oscillations of the transfer probability is significantly affected by the presence of the dot-confined carrier. In particular the Coulomb correlation leads to inelastic scattering. When the inelastic scattering is strong the transmission of electron through the ring is not completely blocked for $(n+1/2)$ magnetic flux quanta.

DOI: 10.1103/PhysRevB.81.165321 PACS number(s): 73.63.Nm, 73.63.Kv, 73.23.Hk

I. INTRODUCTION

Semiconductor quantum rings allow for observation of the electron self-interference. When electron traverses the ring threaded by magnetic field it is subject to a constructive or a destructive interference what manifests itself as conductance oscillations. This effect as predicted by Aharonov and Bohm[1] was observed in many experiments with quantum rings.[2] Manipulation of electron wave function phase in both arms of the quantum ring allows to obtain strong or weak coupling between the ring and the leads by tuning the magnetic field. Recently, besides the most intensively examined two-terminal open quantum rings[3–5] this kind of coupling was experimentally tested in three-terminal[6,7] as well as in four-terminal quantum rings.[8] The current oscillations are highly sensitive to decoherence resulting from interaction with environment such as electron-phonon or electron-electron interactions. Effect of electrostatic interaction on magnetotransport was observed experimentally for ring with quantum dot placed in one of its arms,[9] for ring capacitively coupled to the quantum dot placed beside it[10,11] as well as for rings working in Coulomb blockade regime and confining from few[12] to several hundreds electrons.[13,14] The weak localization theory predicts that the phase coherence time against the effects of the electron-electron interaction approaches infinity for zero temperature.[15] However, besides the decoherence, which is suppressed in low temperature, the electrostatic interaction is also responsible for existence of spatial correlations between charged particles. We may divide correlations induced by electrostatic interaction in a crude way in two types: (i) the Coulomb correlation which introduces dependence of mutual particle positions due to repulsive or attractive interaction and (ii) the Pauli correlation which arises directly from the Pauli exclusion principle. An extremely strong effect of Coulomb correlation on magnetotransport in quantum ring was experimentally observed by Mühle *et al.*[16] Measurements of magnetic field dependence of conductance for system of two concentric capacitively coupled quantum rings revealed two-period oscillations which authors ascribed to existence of the Aharonov-Bohm (throughout this paper we use AB to denote the Aharonov-Bohm effect) effects in the inner and in the external ring. This experiment explicitly proves that Coulomb correlation may greatly affect electron transport in quantum ring even in low temperatures when the decoherence due to electron-electron scattering vanishes.

In this paper we study the single-electron transport through a two-terminal quantum ring in external magnetic field taking into account the Coulomb interaction with another charge carrier. The second particle (electron or hole) is confined within the dot settled in the center of the ring. We assume that the barrier between the ring and the dot is thick enough to neglect the tunnel coupling. For that confinement potential model, we perform time evolution of two-particle wave function by solving suitable time-dependent Schrödinger equation. We observe AB oscillations in the electron transfer probability. We also find that the Coulomb correlation modifies the AB effect in the following way: (i) the maxima of transmission probability grow when transferred electron is attracted by the charged dot while repulsive interaction lowers them and (ii) the probability of electron transfer may grow for $(n+1/2)$ magnetic flux quanta piercing the ring when the interaction is strong enough to excite the carrier that is confined in the inner dot. In the latter case, electron transfers part of its energy to the dot. We find that the energy transfer depends on magnetic field due to both the AB effect and the Lorentz force. The electrostatic interaction causes also positive feedback between transferred electron and the second particle. Even small oscillation of charge in the dot can perturb potential felt by transferred electron which may change the phase of the electron wave function in both ring arms. Finally, an inelastic scattering of electron on oscillating Coulomb potential leads to suppression of AB effect.

The paper is organized in the following way. We define the confinement potential of the considered system and present our theoretical model in Sec. II. Effect of the repulsive as well as effect of the attractive interaction on transmission probability are presented in Sec. III B and in Sec. III C, respectively. Inelastic scattering of the transferred elec-

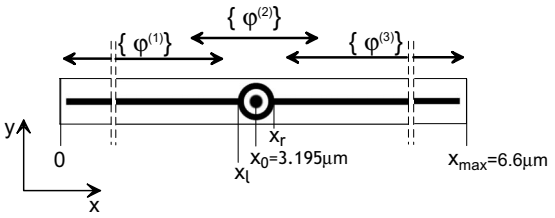

FIG. 1. Confinement potential of two-terminal quantum ring with quantum dot placed inside. Arrows indicate spatial limits of three single-electron wave functions bases used for simulation of electron wave packet in the leads and in the ring (see text below). Labels x_l and x_r mark the left and the right limits of the ring.

tron on Coulomb potential in two-terminal quantum ring is analyzed in Sec. IV. Discussion and conclusions are provided in Sec. V.

II. THEORY

Our confinement potential model consists of quantum ring connected to the left and to the right leads of finite length and a closed circular quantum dot placed in the center of the ring. Tunneling between the ring and the dot is neglected due to wide barrier so that the first particle (electron) can only move in the leads and in the ring while the second (electron or hole) cannot leave the dot. The whole system is put in homogeneous magnetic field which is perpendicular to the quantum ring plane. The confinement potential is schematically depicted on Fig. 1. We assume that the confinement is much stronger in the growth (z) direction than that in (x-y) plane of the ring. Both particles occupy a frozen ground state of the quantization in the growth direction. System of two interacting particles can be described within an effective two-dimensional model. We define the confinement potential in the ring (V_r), in the leads (V_l) and in the dot (V_d) as

$$V_r(\mathbf{r}) = V_e \exp\left(-\frac{||\mathbf{r}-\mathbf{r}_0|-r_r|^p}{\sigma_r^p}\right), \tag{1}$$

$$V_l(\mathbf{r}) = V_e \exp\left(-\frac{|y|^p}{\sigma_r^p}\right), \tag{2}$$

$$V_d(\mathbf{r}) = V_{e(h)} \exp\left(-\frac{|\mathbf{r}-\mathbf{r}_0|^p}{\sigma_d^p}\right). \tag{3}$$

In the above equations $V_{e(h)}$ is the maximal depth of the potential for electron (hole), $\mathbf{r}_0$ is the center position of the ring and the dot, σ_d is the radius of the dot, σ_r is the width of the ring arms and both leads as well, r_r is the radius of the ring. The value of parameter p defines the smoothness of the quantum dot wall. In the calculation we use the following values: V_e=−200 meV, V_h=−140 meV, $\mathbf{r}_0$=[3.195 μm,0], σ_d=55 nm, p=8, σ_r=25 nm, and r_r=130 nm. The length of the left lead is equal to 3 μm while the length of the right lead is 3.2 μm.

The main aim of this work is the investigation of the role of Coulomb correlation in the single-electron transport through the ring. For this purpose we perform the time evolution of two-particle wave function which fulfills the Schrödinger equation

$$i\hbar\frac{\partial}{\partial t}|\Psi(\mathbf{r}_1,\mathbf{r}_2,t)\rangle = \hat{H}|\Psi(\mathbf{r}_1,\mathbf{r}_2,t)\rangle, \tag{4}$$

where the two-particle Hamiltonian is defined as

$$\hat{H} = \hat{h}_1 + \hat{h}_2 + \frac{q_1 q_2}{4\pi\epsilon\epsilon_0 r_{12}}. \tag{5}$$

The Hamiltonians $\hat{h}_1$ and $\hat{h}_2$ are the single-particle energy operators. The third term on the right hand side of above equation describes the electrostatic interaction between the particles which introduces spatial correlations of their mutual positions. We use single-particle Hamiltonians in the following form:

$$\hat{h}_i = \frac{(\hat{\mathbf{p}}_i - q_i\mathbf{A}(\mathbf{r}_i))^2}{2m_i^*} + V_{o(d)}(\mathbf{r}_i), \tag{6}$$

where $\hat{\mathbf{p}}_i = -i\hbar\nabla_{\mathbf{r}_i}$ is the particle momentum operator, m_i^* is effective mass, q_i is the charge of the particle, $\mathbf{A}(\mathbf{r})$ is a vector potential, and $V_d(\mathbf{r}_i)$ is a confinement potential of the dot while $V_o(\mathbf{r}_i)=V_r(\mathbf{r}_i)+V_l(\mathbf{r}_i)$ is a sum of confinement potential of the ring and the leads. Since the tunnel coupling between the ring and the dot is neglected in our theoretical model, the particles confined in spatially separated regions cannot exchange their spins. In other words, the exchange interaction between the electron in the ring and the particle confined in the dot exactly vanishes. Therefore, all the effects due to the presence of the charged dot inside the ring are only result from the Coulomb coupling. For non-negligible tunnel coupling between the ring and the dot the single-particle wave functions of the ring and the dot would overlap. In this case the exchange correlation would lead to a dependence of the transmission probability on the relative spin arrangements. Moreover, for nonzero overlap between the ring and the dot wave functions the particle confined in the dot might be able to tunnel out to the ring.

The Hamiltonian (5) does not depend on the spin coordinates. According to the superposition principle, we expand the correlated wave function of two spinless particles as linear combination

$$\Psi(\mathbf{r}_1,\mathbf{r}_2,t) = \sum_i^M c_i(t)\psi_i(\mathbf{r}_1,\mathbf{r}_2), \tag{7}$$

where $c_i(t)$ are the time-dependent coefficients and M is the size of the two-particle wave functions base. The elements ψ_i are expressed as products of single-particle wave functions

$$\psi_i(\mathbf{r}_1,\mathbf{r}_2) = \varphi_{k(i)}(\mathbf{r}_1)\phi_{m(i)}(\mathbf{r}_2), \tag{8}$$

where every index i corresponds to a particular combination of indices k and m. The k index numbers the states of the first particle which moves in the ring and in the leads while m numbers the states of the second particle in the quantum dot. In order to find the wave functions φ_k and ϕ_m we first express them as linear combinations of centered Gaussian functions. For example, the k-th quantum dot state can be written as

$$\phi_k(\mathbf{r}) = \sum_i a_i^k \exp\left(-\frac{(\mathbf{r}-\mathbf{r}_i)^2}{2\sigma_g^2} - \frac{iqB}{2\hbar}(x-x_i)y_i\right), \quad (9)$$

where a_i^k are the linear combination coefficients, $\mathbf{r}_i=[x_i,y_i]$ are position vectors of Gaussian centers, B is the value of magnetic field and q is the charge of the particle ($+e$ for the hole and $-e$ for the electron). The nodes $\mathbf{r}_i$ form a two-dimensional square mesh with the distance $\Delta_g=\sqrt{2}\sigma_g$ between neighboring nodes. In next step, we diagonalize the single-particle Hamiltonians (6) in the Gaussian functions base (9) in order to find the coefficients a_i^k. In calculations we used material parameters for GaAs, i.e., effective electron mass $m_e^*=0.067m_0$, effective heavy hole mass $m_h^*=0.5m_0$ (m_0 is bare electron mass) and dielectric constant $\epsilon=12.9$. We used nonsymmetric gauge for the vector potential $\mathbf{A}(\mathbf{r})=B[-y,0,0]$ for which the magnetic field vector $\vec{B}$ is parallel to the z axis (perpendicular to the ring plane). The value of parameter σ_g was estimated variationally and was equal to $\sigma_g=5.16$ nm.

We determine the single-particle states in the dot by diagonalizing the single-particle Hamiltonian with confinement potential given by Eq. (3). Therefore, the wave functions ϕ_m were determined only in the quantum dot and in the close surroundings, i.e., in the barrier that separates the dot from the ring. Due to extremely large span of the external subsystem (leads and ring) we divided it into three overlapping parts. In every spatial parts another single-electron wave functions base is introduced, i.e., $\{\varphi^{(1)}\}$, $\{\varphi^{(2)}\}$, and $\{\varphi^{(3)}\}$ as shown on Fig. 1. We find elements of these three bases in a similar way to the one applied for the quantum dot, i.e., diagonalizing the Hamiltonian (6) for confinement potential $V_o=V_r+V_l$. For the preparation of the basis we assumed a different external potential V_o in the three considered regions. In order to determine the basis elements in a region we modified the potential assuming $V_o=0$ outside this region in order to spatially limit the basis wave functions for each region. As the first second and third region (bases $\{\varphi^{(1)}\}$, $\{\varphi^{(2)}\}$, and $\{\varphi^{(3)}\}$) we take $0<x<2865$ nm, 2765 nm$<x<3625$ nm, and 3525 nm$<x<6600$ nm, respectively (see Fig. 1).

Wave functions $\{\varphi^{(1)}\}$ and $\{\varphi^{(3)}\}$ are defined in the left (region 1) and in the right (region 3) leads, respectively, for the distance larger than 200 nm from an outermost parts of the ring (parameters x_l and x_r on Fig. 1). In a similar way, the elements $\{\varphi^{(2)}\}$ are defined in the second region which covers the ring (without a dot) with parts of both leads to the distance of 300 nm from the ring. The ranges of these three regions are schematically marked on a Fig. 1. Notice that the elements of two adjacent basis overlap, e.g., the first with the second as well as the second with the third on the length equal to 100 nm. We carefully checked that these connections do not perturb motion of electron in both channels.[17] For construction of the two-particle wave function (8), we use the lowest energy states obtained from single-particle Hamiltonian diagonalization. In calculations we use $N_d=20$ dot states and $N_1=140$, $N_2=60$ and $N_3=150$ states for bases $\{\varphi^{(1)}\}$, $\{\varphi^{(2)}\}$, and $\{\varphi^{(3)}\}$, respectively.

In the Schrödinger Eq. (4) we substitute for $|\Psi(\mathbf{r}_1,\mathbf{r}_2,t)\rangle$ its expansion (7) and next we multiply both sides of resulting equation by $\langle\psi_k(\mathbf{r}_1,\mathbf{r}_2)|$. We obtain the following matrix equation:

$$i\hbar\mathbf{S}\dot{\mathbf{c}} = \mathbf{H}\mathbf{c}, \quad (10)$$

where $\mathbf{S}$ is the overlap matrix of two-particle wave functions basis elements (8) defined as $S_{km}=\langle\psi_k|\psi_m\rangle$ while $\mathbf{H}$ is the matrix of two-particle Hamiltonian (5) with elements $H_{km}=\langle\psi_k|\hat{H}|\psi_m\rangle$. Details of calculations of the matrix elements of electrostatic interaction are given in previous work.[18] Determination of these matrix elements are very time consuming and therefore we were forced to limit the range of Coulomb interaction in the system. We assume the transferred electron does not interact with the particle confined in the dot if the distance between its position and the dot center exceeds 390 nm. In other words, when electron moves toward the ring it may be partly reflected from a smooth potential step of height $\Delta V=0.28$ meV. The presence of this potential step does not influence the electron transfer probability since the original kinetic energy of electron on Fermi surface ($E_F=1.42$ meV), considered in this work, is several times larger.[19]

The Eq. (10) can be numerically solved by using an iterative method, similarly as was shown in work[20] for time evolution of electron wave packet in a two-terminal quantum ring. Notice however, that every iterative method requires very large number of matrix-vector multiplications so that to retain the stability and to keep the numerical errors as small as possible. Since, the sizes of matrices $\mathbf{H}$ and $\mathbf{S}$ are equal to 7 000, the use of iterative schema in our two-particle problem would be inefficient. Instead, we performed the time evolution of two-particle wave function in another noniterative way. For this purpose, we first diagonalized the two-particle Hamiltonian (5) and put all obtained eigenvectors in columns of the new matrix $\mathbf{U}$ (of the same size as $\mathbf{H}$). Next, we use this $\mathbf{U}$ matrix to perform the unitary transformation of Eq. (10)

$$i\hbar(\mathbf{U}^+\mathbf{S}\mathbf{U})(\mathbf{U}^+\dot{\mathbf{c}}) = (\mathbf{U}^+\mathbf{H}\mathbf{U})(\mathbf{U}^+\mathbf{c}). \quad (11)$$

Let us notice that $\mathbf{U}^+\mathbf{S}\mathbf{U}=\mathbf{I}$ where $\mathbf{I}$ is the unity matrix and $\mathbf{U}^+\mathbf{H}\mathbf{U}=\mathbf{D}$ where $\mathbf{D}$ is diagonal matrix with eigenvalues of energy operator (5) on a diagonal. Due to the diagonal form of both matrices, the system of $M=7000$ coupled equations given by Eq. (10) transforms into system of M decoupled differential equations

$$i\hbar\frac{\partial b_k}{\partial t} = D_{kk}b_k, \quad (12)$$

where $\mathbf{b}=\mathbf{U}^+\mathbf{c}$, with solutions

$$b_k(t) = b_k(t=0)\exp\left(-\frac{iD_{kk}t}{\hbar}\right). \quad (13)$$

Obviously in order to obtain solution for original problem defined by Eq. (10), i.e., to obtain values of coefficients c_k, one performs a backward transformation $\mathbf{c}=\mathbf{U}\mathbf{b}$. We made the diagonalization of $\mathbf{H}$ numerically. Therefore, in order to estimate the numerical errors which may appear due to performing the unitary transformation, we always checked the energy and the norm conservation for two-particle wave

function. The relative errors do not exceed 10^{-6}.

For $t=0$ we use the following form for the initial two-particle wave function:

$$\Psi_s = \Psi(\mathbf{r}_1,\mathbf{r}_2,t=0) = \varphi_0(\mathbf{r}_1)e^{ik_0x_1}\phi_0(\mathbf{r}_2). \tag{14}$$

Wave function $\phi_0(\mathbf{r}_2)$ describes the particle (electron or hole) confined in the dot in the ground state while $\varphi_0(\mathbf{r}_1)e^{ik_0x_1}$ is the wave function of the electron moving in the left channel toward the ring with the average momentum depending on k_0 value. We determined $\varphi_0(\mathbf{r}_1)$ by diagonalizing the Hamiltonian (6) in the centered Gaussian functions base (9) with the confinement potential

$$V_s(\mathbf{r}) = V_l(\mathbf{r}) + \frac{m_e^*\omega^2}{2}(x-x_s)^2, \tag{15}$$

where x_s is the center position of harmonic oscillator in the left channel. It was situated in the distance of 995 nm from the center of the ring (dot). The strength of the harmonic oscillator depends on the oscillator length (l_e), i.e., $\hbar\omega = \hbar^2/m_e^*/l_e^2$. In calculations we used $l_e=50$ nm. Such way of determination of φ_0 inherently includes the magnetic translation phase change. For $t=0$ we give the electron in the left channel momentum $\hbar k_0$ with $k_0=0.05/\mathrm{nm}$ which corresponds to the average energy on the Fermi surface ($E_F=1.42$ meV) in the two-dimensional electron gas with density[20] $n=4\times10^{10}/\mathrm{cm}^2$. The choice of initial conditions, i.e., values of parameters such as x_s or l_e is quite arbitrary. In Sec. III C we will shortly comment the results obtained also for other sets of initial parameters.

III. RESULTS

Below we denote by P_A, P_B, and P_C the probabilities of finding the transferred electron in the left channel, within the ring and in the right channel, respectively. For these quantities we defined auxiliary operators

$$\hat{P}_A = \Theta(x_l - x_1), \tag{16}$$

$$\hat{P}_B = \Theta(x_1 - x_l) + \Theta(x_r - x_1) - 1, \tag{17}$$

$$\hat{P}_C = \Theta(x_1 - x_r). \tag{18}$$

In the above definitions $\theta(x)$ is the Heaviside function while $x_l=3040$ nm and $x_r=3350$ nm are the left and the right limits of the ring in x direction, respectively, as shown on Fig. 1. Each P_i can be simply computed at any time as expectation value of specific operator $\hat{P}_i$, i.e., $P_i(t) = \langle\Psi(\mathbf{r}_1,\mathbf{r}_2,t)|\hat{P}_i|\Psi(\mathbf{r}_1,\mathbf{r}_2,t)\rangle$ (for $i=A,B,C$). We treat P_C and P_A are lower bounds for probability of electron transfer and backscattering, respectively, since the ring is not completely empty at the end of simulations. A part (less than 5%) of the packet always stays inside the ring since the sizes of the channels are limited.

A. Electron transfer without interaction

We start the presentation by the case when the transferred electron does not interact with the charged dot. These results will serve as the reference point for the main calculation where the interactions are included. Electrostatic interaction was turned off simply by extracting its matrix elements from two-particle Hamiltonian (10). The probability distributions P_A, P_B, and P_C as functions of time and magnetic field for this case are depicted on Fig. 2.

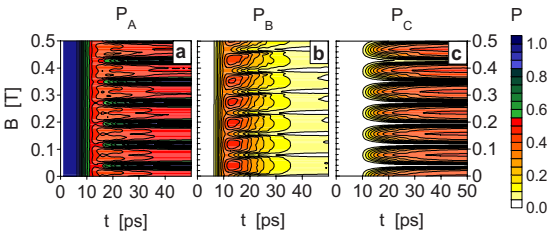

FIG. 2. (Color online) Probabilities P_A, P_B, and P_C as functions of time and magnetic field. Coulomb interaction between transferred electron and charged dot is neglected.

All probabilities strongly oscillate with magnetic field which is a typical manifestation of Aharonov-Bohm effect. Period of these oscillations is $\Delta B=78$ mT. This value is close to $\Delta B_T=77.98$ mT obtained for the one-dimensional ring from formula

$$\Delta B_T = \frac{h}{e}\frac{1}{\pi r^2} \tag{19}$$

for ring radius $r=130$ nm. Especially the most intensive AB pattern is visible for the probability of electron transfer [see Fig. 2(c)], i.e., distinct maxima for multiple integers of magnetic field flux quanta [$\phi_n=n(h/e)$ with $n=0,1,2,\ldots$] and blockades of electron transfer in the half way between adjacent maxima. The presented time-magnetic field characteristics of probabilities clearly show the dynamics of wave packet motion. For the first 6 ps the most energetic part of the electron wave packet reaches the left entrance to the ring but then it takes it about 4 ps to get through the ring to the second junction. This is visible as a large growth of P_C value on Fig. 2(c) for $t\approx10$ ps. One can also see that the electron wave packet leaves the ring more quickly when the P_C is close to its maximum rather than for its minimum. Besides the AB effect, probabilities of finding the electron in the left and in the right leads depend also on magnetic field due to the Lorentz force.[20] In order to show magnetic field effect on electron transport, we made the cross sections of P_A, P_B, and P_C distributions shown on Fig. 2 for $t=50$ ps. These cross sections are shown on Fig. 3(a). One may notice that the electron transfer through the ring is completely blocked due to AB effect only in low magnetic field. For example, for $B=39$ mT probability of an electron transfer is of the order 10^{-4}. However, for high magnetic field, the probability of electron transfer does not drop to zero at all. It means that the AB effect is perturbed by the Lorentz force. Due to the narrow cross sections of leads and arms of the ring there are no significant changes in the maxima of transmission probability as it was theoretically predicted[20] and experimentally observed[6] for rings with wider arms.

Figure 3(a) shows also comparison of results obtained for 100 nm and for 200 nm wide overlap regions. Probabilities

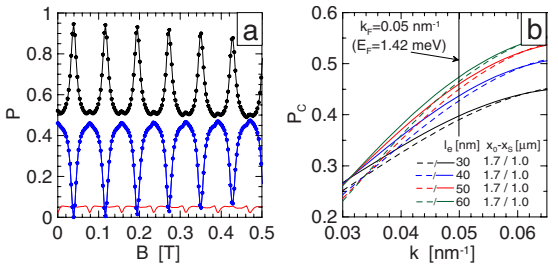

FIG. 3. (Color online) a) Probabilities P_A (black), P_B (red), and P_C (blue) as functions of magnetic field for $t=50$ ps. Elements of bases $\{\varphi_1\}$ and $\{\varphi_2\}$ as well as elements of $\{\varphi_2\}$ and $\{\varphi_3\}$ overlap on the length of 100 nm (solid lines) and 200 nm (dots). b) Probability of electron transfer as a function of the initial wave vector k_0 for several combinations of parameters l_e and x_s defining the shape of single-electron wave packet and its center position for $t=0$. In both cases, the electron does not interact with charged dot.

P_A and P_C are the same what proves that electron may smoothly move between neighboring regions without reflection. In order to check the influence of initial conditions on the probability of electron transfer we made additional simulations for several different values of initial parameters that is for k_0, l_e, and x_s. Results are presented on Fig. 3(b). We see that the probability of electron transfer strongly depends on the spatial spread of original wave packet and its initial momentum rather than its distance from the ring. When initial wave packet becomes wider (value of l_e is larger) then the probability of electron transfer grows even by several percents. On the other hand, transmission probability is less susceptible for change in the distance between initial position of wave packet and center position of the ring. Results obtained for 1.7 and 1 μm are very much the same, i.e., the difference is only about 1%.

B. Effect of repulsive interaction on electron transport

In order to investigate the correlation effects which are due to the repulsive interaction, we put single electron into the dot and turned on the interaction in the system. Transferred electron feels a growing repulsive electrostatic potential as it approaches the ring. Probabilities P_A, P_B, and P_C as functions of evolution time and magnetic field obtained for this two-electron system are shown in Fig. 4. Comparison of probabilities distributions obtained for electron subject to the repulsive interaction [Figs. 4(a)–4(c)] with those obtained for noninteracting electrons [Fig. 2] allows us to distinguish several differences between these two cases. Maxima of transmission probability are decreased for repulsive interaction in relation to the previous case. Consequently, the interaction is also responsible for the growth of probability of finding the electron in left lead P_A [cf. Figures 2(a) and 4(a)] and also for faster electron wave packet leakage from the ring for $t>40$ ps. However, the interaction does not change the period of AB oscillation. The probabilities P_C shown on Fig. 2(c) and on Fig. 4(c) change with the same frequency. For quantitative analysis of interaction influence on P_A, P_B, and P_C we have made the cross sections of probabilities distributions for $t=50$ ps. These cross sections are presented on Fig. 5(a).

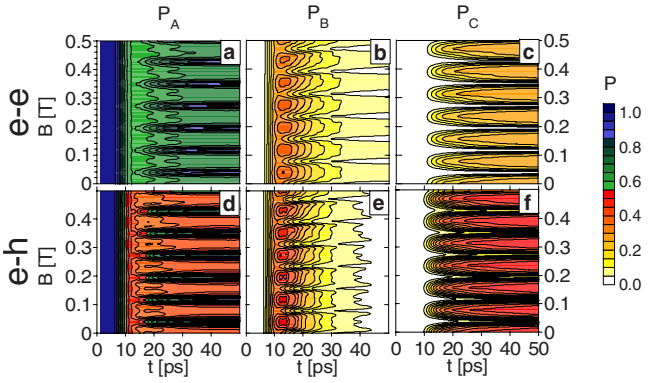

FIG. 4. (Color online) Probabilities P_A, P_B, and P_C as functions of time and magnetic field for the case when the transferred electron electrostatically interacts with charged dot. The figures (a–c) were obtained for repulsive interaction (electron confined in the dot) while figures (d–f) for attractive interaction (heavy hole confined in the dot).

Comparison of P_C cross sections shown on Figs. 3(a) and 5(a) reveals that repulsive interaction is responsible for about 10% decrease in transmission probability. It results from the fact that when electron approaches the ring, it simultaneously climbs on a growing slope of the Coulomb potential of the second electron and converts part of its kinetic energy into potential energy. Therefore, the electron wave packet enters the ring with lower average wave vector k than its initial value k_0. Since the probability of electron transfer strongly depends on the k value [see Fig. 3(b)], the lower average k value bring the transmission probability down. Such situation is clearly visible on Fig. 3(b) for $k_0<k_F$. In order to check this hypothesis we performed additional time evolution of two-electron wave function giving the transferred electron higher initial momentum just enough to overcome

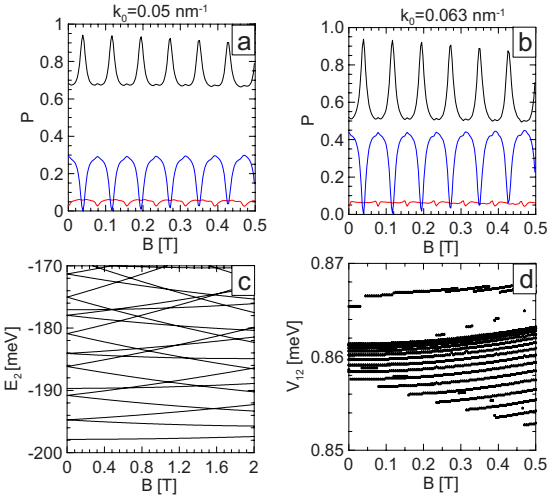

FIG. 5. (Color online) Probabilities P_A (black line), P_B (red line), and P_C (blue line) as functions of magnetic field for $t=50$ ps and for (a) $k_0=0.05$ nm^{-1} and (b) $k_0=0.063$ nm^{-1}. The transferred electron interacts electrostatically with negatively charged dot. (c) Energy spectrum of single electron confined in the dot. (d) Interaction energies for the lowest-energy states of two electrons confined in closed quantum ring–quantum dot system.

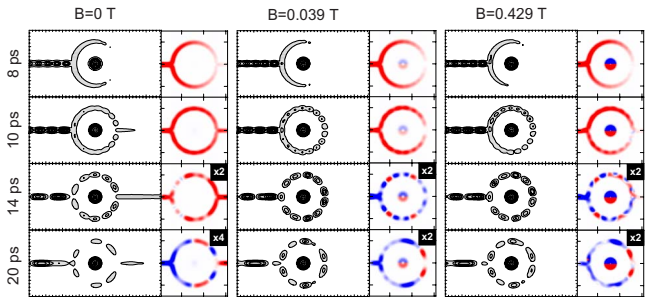

FIG. 6. (Color online) Two-electron probability density (odd columns) and current density (even columns) calculated for $t=8$, 10, 14, 20 ps. The red color indicates the current flowing to the right lead while the blue color marks the current flowing to the left. Intensity of the colors is proportional to the amplitude of current. The color scales for two lowest rows are enhanced by the multipliers which are shown in top right corners.

the repulsive interaction [see Fig. 5(b)]. We assumed 0.86 meV as average value of interaction energy what gives initial momentum $k_0=0.063$ nm^{-1} and corresponds to $E_F=2.28$ meV. Probabilities P_A, P_B, and P_C as functions of magnetic field for this case for $t=50$ ps are presented on Fig. 5(b). We notice that this picture is almost identical with results obtained for electron transport without interaction [cf. Figures 3(a) and 5(b)]. As one may notice, the repulsive interaction does not change the frequency of AB oscillations [cf. Fig. 3(a) and 5(b) with Fig. 5(a)]. This results from the fact that we did not include the term describing interaction between the magnetic dipole moments in the two-particle Hamiltonian (5). In addition, the electrostatic potential originated from charged dot is too weak to induce the electron density redistribution along the ring radius and thus do not change the effective ring radius [see Eq. (19)]. In order to get a deeper insight into the dynamics of the two-electron wave packet we have calculated the total two-electron probability densities and the current densities. Results obtained for $t=8,10,14,20$ ps are shown on Fig. 6. When the magnetic field is absent in the system, the total electronic density as well as the current remain symmetrical relative to $y\rightarrow -y$ reflection during the whole time evolution. Obviously, it results from the fact that the electrostatic interaction term in two-particle Hamiltonian (5) preserves this symmetry and thus does not change the symmetry of the two-particle wave function. A detailed analysis of the currents for $B=0$ reveals that the electrostatic interaction does not induce current inside a dot as one at first may expect. When electron approaches the ring, both electrons repel each other into opposite directions. As we do not see any current induced in the dot for $B=0$, we can state that the electron confined in the dot does not react to the presence of the first electron. This lack of reaction of the second electron stems from the fact that the interaction is small in comparison with the lowest single-electron energy excitations in the dot. We see in Fig. 5(d) that the value of interaction energy between two electrons confined in closed quantum ring–quantum dot structure is about 0.86 meV. On the other hand, the energy spacings between the first two excited states and the ground state in quantum dot confining single electron [see Fig. 5(c)] are equal to 3.1 meV for $B=0$. The interaction energy is more than three times smaller than even the lowest two single-electron energy excitations and therefore can hardly mix the quantum dot states. Since the transferred electron cannot excite the second electron, there is no energy transfer to the dot. Transferred electron scatters only elastically on the statical repulsive potential created in the leads and in the ring by second electron which is confined in the inner dot. The magnetic field breaks the symmetry of the confinement potential and favors an upper arm. The larger part of electron wave packet is directed to this arm [see Fig. 6 for $B=0.039$ T and $B=0.429$ T]. Let us notice that the current in the dot is more intensive for stronger magnetic field. Since the electrostatic interaction is too weak to induce it, only the external magnetic field may be responsible for its existence. We explain it by analyzing the matrix elements of probability current

$$\mathbf{j}_{km}=\frac{i\hbar}{2m^*}(\phi_m\nabla\phi_k^*-\phi_k^*\nabla\phi_m)-\frac{q}{m^*}\mathbf{A}\phi_k^*\phi_m. \quad (20)$$

The first component on the right hand side in Eq. (20) is the paramagnetic part of current while the second component is diamagnetic. Now, if we notice that electron occupies exclusively the ground state of s symmetry for $B=0$ we see that the paramagnetic current completely disappears.[21] One may notice on Fig. 5(c) that even for $B=0.5T$ the energy spacings between the first excited state and the ground state ($E_1-E_0=2.7$ meV) are still much larger than interaction energy. Since the interaction is not able to mix the dot states, the electron confined in the dot still occupies the ground state and there is no paramagnetic contribution to the current even in high magnetic field. Since the diamagnetic current depends on product of probability density and magnetic field, its contribution increases for stronger magnetic field what is clearly visible when comparing dot currents depicted in the fourth and in the sixth columns on Fig. 6.

C. Effect of attractive interaction on electron transport

In the preceding section we showed that the repulsive interaction is responsible for decrease in probability of electron transfer through the ring. When electron approaches the ring and negatively charged dot, it is scattered elastically on a static potential. A part of the electron kinetic energy is converted into the potential energy. The average momentum of the packet is decreased, which leads [Fig. 3(b)] to a decrease in probability of electron transfer. Let us notice that this mechanism may presumably lead to an increase in the transmission probability provided that the electron is attracted by the positively charged dot. In order to check this conjecture we put the heavy hole in the dot and made time evolution of wave function for this electron-hole system. Probabilities P_A, P_B, and P_C distributions as functions of evolution time and magnetic field obtained for this case are shown on Figs. 4(d)–4(f). Comparison of the results obtained for the repulsive interaction [Figs. 4(a)–4(c)] with those obtained for the attractive one [Figs. 4(d)–4(f)] shows that the probability of electron transfer through the ring is indeed larger in the latter case. Moreover, when the transferred electron feels the presence of the positively charged dot it spends

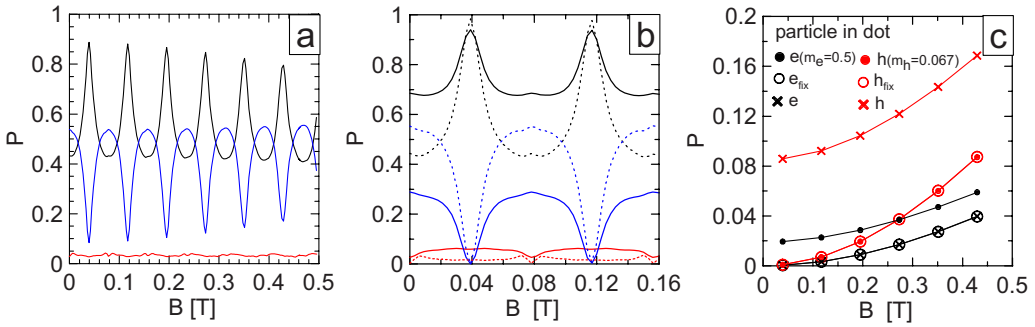

FIG. 7. (Color online) Probabilities P_A (black), P_B (red), and P_C (blue) as functions of magnetic field calculated for a system: (a) with positively charged dot and (b) with electron or hole frozen in the dot ground state (solid line for electron and dotted one for hole). (c) Effect of Coulomb correlation in the dot on probability of electron transfer for $B=(n+\frac{1}{2})\Delta B$ with integer n. In (c) the dot is occupied by electron (black color) or by hole [gray (red color)]. Lines are guide to the eye.

less time in the ring. Attractive interaction leads to an increase in the packet average momentum and velocity. Therefore, the electron traverses the ring in shorter time than in the case when it is repelled by negatively charged dot. Cross sections of those probabilities distributions depicted in Fig. 7(a) indicate that the AB oscillations are independent of electrostatic interaction. Probabilities P_A and P_C oscillate with the same frequency as those shown on Fig. 5(a) obtained for repulsive interaction, the period of AB oscillation is still equal to $\Delta B=78$ mT. The electrostatic interaction does not change the frequency of AB oscillations but may significantly influence the electron transfer probability provided that the confinement along the ring radius is strong. The change of character of electrostatic interaction from repulsive to attractive makes the maxima of probability of electron transfer grow by more than 20%. Repulsive or attractive potential changes the wave vector distribution in the electron wave packet due to its deceleration or acceleration by the electrostatic potential. As it is clearly visible on Fig. 3(b) such a change in the average value of electron wave vector should influence, to a large extent, the probability of the electron transfer. However, when the electron interacts with a positively charged dot, the minima of the transfer probability at half flux quanta become shallower. For example, for $B=39$ mT, transmission probability falls only to 8.4% while the electron transfer is completely blocked when the electron does not interact with particle confined in a dot [Fig. 3(a)] or is repelled by a negatively charged dot [Fig. 5(a)]. Since the Lorentz force is negligible for low magnetic field, this AB blockade weakness stems only from the interaction of electron wave packet with the positively charged dot. Figure 7(b) shows probabilities obtained for attractive and repulsive interaction between the transferred electron and the second particle which is frozen in the ground state in the dot. Electron or hole confined in the dot cannot move and thus we may neglect the correlation effects in the dot. Despite this fact, the two-particle wave function is still partly correlated since the transferred electron interacts with charged dot and its behavior depends on the distance from the dot due to the Coulomb interaction. We see on Fig. 7(b), that electron cannot be transferred through the ring for $\Delta B/2$ independently of the character of electrostatic interaction. It means that the Coulomb correlation in the dot is entirely responsible for the weakness of AB blockade for low magnetic field. Comparison of the results shown on Figs. 5(a) and 7(a) suggest that the effect of Coulomb correlation on transmission probability also depends on the effective mass of particle confined in the dot. We demonstrate this dependence on Fig. 7(c) for electron (black crosses), frozen electron (black empty circles), and electron with large effective mass ($m_e^*=0.5$ (black dots) as well as for hole [gray (red) crosses], frozen hole [gray (red) empty circles], and hole with small effective mass ($m_h^*=0.067$ [gray (red) dots] confined in the dot. The results for the frozen hole and the hole with a small mass are identical. This shows that small effective mass prevents particle from moving inside the dot regardless of the character of electrostatic interaction. For heavier particle, i.e., electron or hole confined in the dot with effective mass of about 0.5, probability of electron transfer for $B=39$ mT is increased. However, this growth is bigger for the attractive (8%) than for the repulsive (2%) interaction. Notice also that the transmission probability grows faster for the attractive interaction than those for the repulsive one.

Relatively large effective mass of the heavy hole leads to its stronger localization in the dot. This results in smaller spacings between the lowest energy levels than those for electron [cf. Figure 8(a) for hole and Fig. 5(c) for electron]. For the hole confined in the dot, these spacings are comparable with the average absolute value of the attractive interaction. For example, in the absence of magnetic field, the two lowest excited states shown on Fig. 8(a) lie only 0.59 meV above the ground state while the absolute average value of interaction energy between electron and hole shown on Fig. 8(b) for closed quantum dot–quantum ring system is

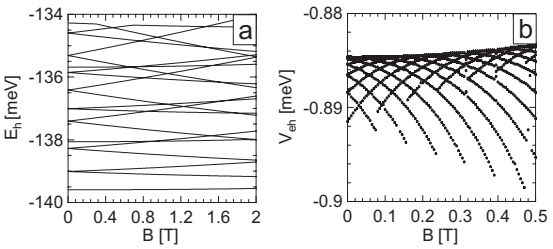

FIG. 8. (a) Energy spectra of heavy hole confined in the dot and (b) electron-hole interaction energy in closed quantum ring–quantum dot system.

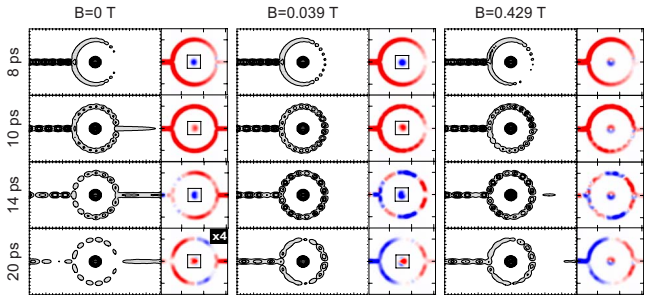

FIG. 9. (Color online) The electron-hole probability density (odd columns) and current density (even columns) for $t=8$, 10, 14, 20 ps. Red and blue colors indicate directions of current flow, to the right and to the left, respectively. Intensity of colors are proportional to the amplitudes of currents. The scale for the currents in the dot was enhanced four times (square region) for $B=0$ and $B=39$ mT.

about 0.885 meV. Therefore, when the transferred electron approaches the positively charged dot placed in the center of the ring, it may quite easily excite the hole in the dot.

Figure 9 shows the total probability density and current density distributions obtained for fully correlated electron-heavy hole system. For $B=0$ and $t=8$ ps, when the electron enters the ring through the left junction, the hole is attracted by the electron and starts to move which induces the current in the dot. At first, this current flows to the left (blue color on Fig. 9), but when the electron fills more or less equally the ring ($t=10$ ps) which makes the potential in the dot less perturbed, the hole reflects from the wall. Then the current within the dot flows to the right (red color). The hole is excited in the dot and starts to oscillate. Its spatial oscillation do not fade out even for long time, e.g., $t=20$ ps. This indicates that when the electron passes through the ring, it transfers part of its energy to the dot. As the energy of the electron changes permanently, we may state that it scatters inelastically on the Coulomb potential generated by the oscillating hole. Similar oscillations of current in the dot in the horizontal direction are also visible for $B=39$ mT (fourth column on Fig. 9). We will analyze in detail this process of energy transfer between the electron and the dot in next section.

Horizontal oscillations of the hole in the dot perturb the potential in both arms of the ring. Although, the confinement potential of the ring is perturbed, it remains symmetrical relative to $y \rightarrow -y$ reflection. That produces identical phase shifts in both parts of electron wave packet, i.e., in the upper and in the lower ring arms. In other words, the weakness of AB blockade observed on Fig. 7(a) is not a result of dephasing[15] because the phases in the upper and in the lower parts of the electron wave packet still change coherently. In consequence, when they meet at the second junction for $B=(n+1/2)\Delta B$, their phase difference is no longer equal to π due to potential perturbation. This effect was recently predicted by Chaves *et al.*[22] They obtained very similar dependence of transmission probability on magnetic field to that shown on Fig. 7(a) for an open two-dimensional ring with two static impurities put near both arms of the ring and placed symmetrically to its center.

For high magnetic field, e.g., $B=0.429$ T (the last column on Fig. 9), these current oscillations become invisible and

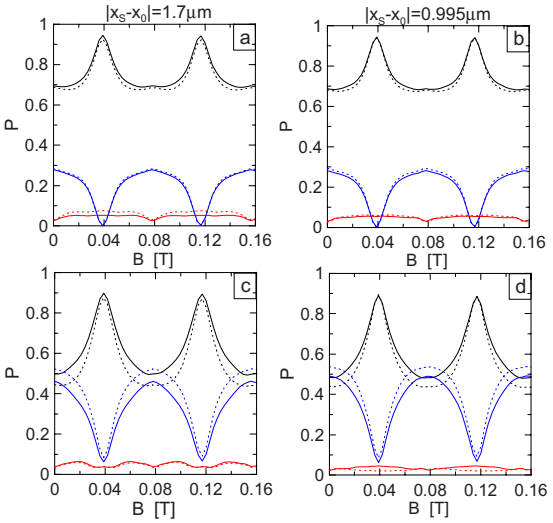

FIG. 10. (Color online) The P_A (black), P_B (red), and P_C (blue) probabilities as functions of magnetic field for four combinations of $|x_S-x_0|$ and l_e initial parameters. Results were obtained for $t=50$ ps. Pictures (a) and (b) are for repulsive interaction while (c) and (d) are for attractive interaction. Solid lines are for $l_e=30$ nm and dotted for $l_e=50$ nm.

now the current encircles the dot in the clockwise direction, i.e., in the opposite direction to the one of the last column of Fig. 6 when electron occupies the dot. It does not mean that the oscillations entirely disappear, but only the diamagnetic contribution to the current in the dot is much larger than paramagnetic contribution. Such large diamagnetic current was also induced by magnetic field when an electron was confined in the dot. However, if we compare the dot currents in the last columns of Fig. 6 and of Fig. 9 we will see that the current is less intensive for the hole (color scales on both figures are the same). To explain this fact we make an assumption that the densities of electron and hole in the dot do not differ much for the same magnetic field which seems reasonable for our case, since the confinement potential of the dot is quite strong. With this assumption, and for fixed value of magnetic field, the absolute value of diamagnetic term in Eq. (20) depends only on the effective mass of particle. Since the diamagnetic current is inversely proportional to the effective mass and the effective mass of the electron used in calculation was about $m_h/m_e=7.5$ times smaller than effective mass of the heavy hole, the diamagnetic contribution to the current is by about m_h/m_e larger for the electron than that for the hole.

Probability of electron transfer depends also on the initial conditions which we have assumed quite arbitrarily. In order to check the sensitivity of the transmission probability to initial conditions, we studied the time evolution of the two-particle wave function (7) for four combinations of the distance between the initial position of electron wave packet and the center position of the ring ($|x_s-x_o|$) and its spatial span l_e. Probabilities P_A, P_B, and P_C calculated for these new initial parameters and for $t=50$ ps are shown in Figs. 10(a)–10(d). If the transferred electron interacts with negatively charged dot, these probabilities are only slightly sensitive to the change of the initial conditions [see Figs. 10(a)

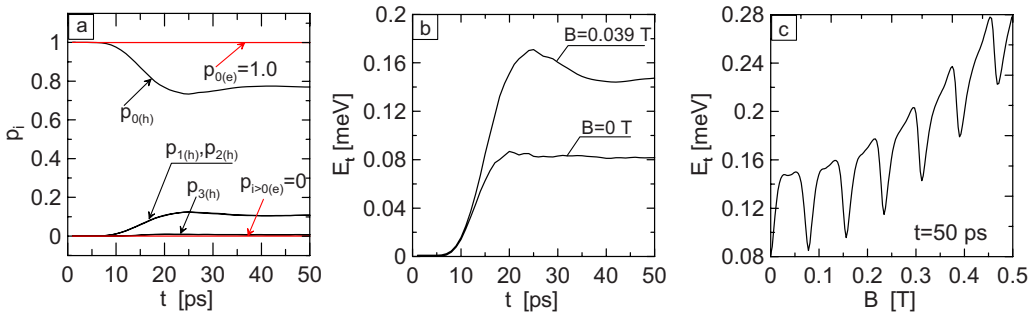

FIG. 11. (Color online) (a) Probabilities of occupation of the low-energy quantum dot states by the electron (red) and by the hole (black) as functions of the evolution time. In (a) results were obtained for $B=39$ mT. (b) Energy gained by the hole confined in the dot as function of time. (c) Permanent energy transfer to positively charged dot depending on magnetic field.

and 10(b)]. For example, transmission probability increases only about 1% when the parameter l_e changes from 30 to 50 nm for $|x_s-x_o|=0.995$ μm. Much larger differences in transmission probability were found for system with the positively charged dot. Generally, the amplitude of AB oscillations is larger for larger l_e and when the electron wave packet stays closer to the ring for $t=0$. For example, for $B=0$ and $|x_s-x_o|=1.7$ μm, the transmission probability grows from about 0.46 for $l_e=30$ nm to about 0.52 for $l_e=50$ nm what gives the growth of about 6% while it is equal to about 4.7% for $|x_s-x_o|=0.995$ μm. When the parameter l_e is fixed, then the change in $|x_s-x_o|$ value make less impact on the transmission probability. For example, for $l_e=30$ nm, we get the increase in transmission probability of about 3% when the initial position of the electron wave packet is shifted by about 0.7 μm closer to the ring whereas for $l_e=50$ nm the increase in P_C value is less distinct and is equal to about 1.1% then. On the other hand, weakness of AB blockade for electron-hole system is independent of the initial position of transferred electron wave packet but grows by 2% when the value of parameter l_e changes from 30 nm to 50 nm for $B=39$ mT.

IV. ELASTIC AND INELASTIC SCATTERING

In the previous section we showed that during the electron transition through the ring, the particle confined in the dot may start to move. Its spatial oscillations within the dot are induced by the electrostatic interaction between charged particles and are due to the excitation to the higher energy states in the dot. During the process of excitation, the transferred electron loses a part of its kinetic energy which is gained by the second particle. If this energy loss is permanent, i.e., the electron does not recover it after it leaves the ring, then the process of electron scattering on the Coulomb potential is inelastic. Figure Fig. 11(a) shows the probabilities of occupation of the low-energy quantum dot states as functions of evolution time. This picture was obtained for $B=39$ mT. In order to find the probability of occupation of the particular dot state we have projected the two-particle wave function (7) on that state

$$p_i(t) = \langle \Psi(\mathbf{r}_1,\mathbf{r}_2,t)|\hat{p}_i|\Psi(\mathbf{r}_1,\mathbf{r}_2,t)\rangle, \tag{21}$$

where $\hat{p}_i=|\phi_i\rangle\langle\phi_i|$ is the projection operator.

When electron is confined in the dot the probabilities of occupation of the dot states do not change in time. For the confinement potential model considered here, the electron is always in the ground state. As it was mentioned in Sec. III B the electrostatic interaction is too weak to excite the electron within the dot and this is the reason we do not see any current in the dot on Fig. 6 for $B=0$. Situation changes dramatically if we consider the hole confined in the dot. We see on Fig. 11(a) that after a few ps, the hole starts to be excited since the probabilities of two the lowest excited states with angular momentum $L=1$ grow with time. Contributions of these states are identical, since their linear combination gives the hole oscillation in the horizontal direction. Obviously, it results from the symmetry of the confinement potential model relative to $y\rightarrow -y$ reflection and due to the absence of Lorentz force in the system for such small magnetic field. Other hole states in the dot remain unoccupied. The process of the hole excitation ends up for $t=25$ ps. During the next 15 ps, the hole partly de-excite and the probability of finding it in the ground state is increased. For $t>40$ ps, contributions from the low-energy dot states stabilize. These changes of probabilities of occupation of the dot states influences the energy of the hole. We calculated the energy gained by hole, i.e., energy transfer to the dot, from following formula:

$$E_t(t) = \sum_{i=0}^{19} p_i(t)E_i^{\mathrm{dot}} - E_0^{\mathrm{dot}}, \tag{22}$$

where E_i^{dot} are the eigenenergies of particle confined in the dot. Figure 11(b) shows the time characteristics of the energy transferred to the dot which is occupied by the hole for $B=0$ and $B=39$ mT. We see that both cases differ qualitatively as well as quantitatively. In the absence of magnetic field, the energy is transferred to the dot for $t<20$ ps. Then the hole energy changes only slightly and for $t=50$ ps it stabilizes at about 0.08 meV. Thus, the transferred electron lose 5.6% of its original kinetic energy. For $B=39$ mT the energy transfer in the first 25 ps is twice of that observed for $B=0$. Next, the hole gives back a part of the gained energy to the electron but for $t=50$ ps is still much larger than in the case for $B=0$. The occurrence of such a distinct difference in energy transfer is not incidental. The magnetic field dependence of the energy transferred to the dot occupied by the hole, depicted on Fig. 11(c), indeed have minima for $B=n\Delta B$, i.e.,

for maxima of the transmission probability. On the other hand, the maxima of the energy transfer do not appear exactly for $B=(n+1/2)\Delta B$, as one may expect, but they are shifted toward higher magnetic fields. On Fig. 11(c), we see that, besides the oscillatory character of magnetic field dependence of energy transfer what is the signature of AB effect, the minima and maxima of energy gained by the hole lie higher in energy when magnetic field becomes stronger. This nonlinear effect is the signature of presence of magnetic force in the system. Magnetic field breaks the symmetry of the confinement potential of the ring and consequently the Lorentz force injects larger part of the electron wave packet to the upper arm of the ring (see density distributions on Figs. 6 and 9 for $B=0.429$ T and $t=8$ ps). In this case, the magnitude of Coulomb interaction between both particles is getting stronger. It results in a larger amount of the energy transferred to the dot. For example, for $B=0.453$ T the energy gained by the hole reaches even 0.278 meV what is 19.5% of original kinetic energy of the transferred electron.

V. DISCUSSION AND CONCLUSIONS

The presence of a charged dot in the center of the ring significantly influences the probability of electron transmission. The maxima of transmission probability observed in the Aharonov-Bohm effect are shifted down (up) for repulsive (attractive) interaction between transferred electron and the charged dot [cf. Fig. 3(a) for empty dot with Figs. 5(a) and 7(a)]. The reduction in transmission probability stems from lowering the average value of wave vector in the electron wave packet [see Fig. 3(b)] due to deceleration of its motion when it moves toward the ring. The magnitude of this probability reduction depends in particular on the radius of the ring and on the number of particles confined in the dot. Interaction should be stronger for smaller rings due to stronger Coulomb coupling of the ring and the dot, and for multiple charged dot. Moreover, the probability of electron transmission may also be decreased when the kinetic energy of electron is of the same order as the interaction energy. Then, the low-energy part of the electron wave packet should be reflected back from repulsive Coulomb potential before it get closer to the ring.

The single-electron transport in quantum ring depends strongly on the relations between the magnitude of interaction energy and the lowest excitation energies of particle confined in quantum dot. When the spacings between the two lowest excited states and the ground state in the dot are several times larger than the interaction energy [cf. Figs. 5(c) and 5(d)], the electron transport through the ring is blocked for $(n+1/2)\phi_0$ flux quanta in low magnetic field [see the magnetic field dependence of P_C (blue color) on Figs. 5(a) and 5(b)]. In this case, the transferred electron is not able to excite the second particle which stays in the ground state [the p_i do not change for repulsive interaction (red color) on Fig. 11(a)] and the Coulomb potential originated from charged dot keeps its azimuthal symmetry. In consequence, the quantum interference is not perturbed by the interaction because the transmitted electron scatters elastically in quantum ring, i.e., there is no permanent energy transfer between the electron and the charged dot.

The situation changes significantly when the interaction energy becomes comparable to excitation energies. For example, the magnetic field dependence of transmission probability obtained for attractive interaction and presented on Fig. 7(a) reveals AB blockade weakness for $(n+1/2)\phi_0$ even for low magnetic field. The heavy hole is excited by the transferred electron due to their Coulomb interaction [see p_i for attractive interaction (black color) on Fig. 11(a)], and starts to oscillate horizontally within the dot [see the currents on Fig. 9 for $B=0$ and $B=39$ mT]. Coulomb potential originated from oscillating hole charge, breaks the azimuthal symmetry of the confinement potential in the ring. This dynamical charge redistribution inside the dot perturbs the quantum interference in the ring. Electron scatters inelastically on the oscillating Coulomb potential which changes coherently the phase of the electron wave packet in both arms of the ring. Finally, this leads to the suppression of AB effect, i.e., the maximum-to-minimum ratio is decreased but the amplitude of transmission probability does not change much. Interestingly, the energy gained by the charge confined in the dot shows strong oscillation in the magnetic field [see Fig. 11(c)]. Maxima are localized in the proximity of $(n+1/2)\phi_0$ and are slightly shifted toward the higher magnetic fields.

Generally the AB oscillation period depends on: (i) the effective radius of the ring and (ii) the vector potential. Oscillation of charged particle within the dot creates an additional magnetic field and vector potential. However this induced magnetic field is very small,[21] i.e., of the order of few hundreds nT and therefore this effect cannot perturb significantly the AB period. The Coulomb interaction may potentially influence the effective ring radius since the electron tends to move closer to the positively charged dot due to attractive interaction whereas it tries to keep away from negatively charged dot due to repulsive interaction when it traverses the ring. However the effective ring radius can be changed only if the interaction is strong enough to modify the electron density along the ring radius what is possible for very wide ring arms. For confinement potential model considered here, the interaction is too weak to make noticeable redistribution of electron density in the ring and we did not observe any change in AB period due to the Coulomb interaction.

Similar effect, i.e., suppression of AB oscillation in conductance was observed in experiment of Mühle[16] for two capacitively coupled quantum rings. They obtained much less distinct AB oscillations for outer ring than the conductance oscillation arising from AB effect for the inner ring. The authors ascribes this effect to the imperfections of the confinement potential of the outer ring. However it does not explain such large amplitude of oscillation induced by the inner ring since the charge redistribution in the inner ring perturbs the Coulomb potential felt by electrons in the outer ring. In our opinion besides the imperfections of the outer ring, the difference in amplitudes of AB oscillations observed in experiment results also from inelastic scattering of the transferred electrons on the Coulomb potential. Since the energy gaps between the ground state and the first excited state are much smaller in the ring than in the dot, the particle confined in the inner ring should be much more easily ex-

cited, i.e., much energy may be transferred to the inner ring than to the dot. In such a case, strong spatial oscillations of particle within the inner ring may govern the motion of the electron injected to the outer ring. Finally, this strongly inelastic scattering process can suppress the AB oscillation of the outer ring rather than the amplitude of the electron transmission probability.

In conclusion, the effect of Coulomb correlation on single-electron transport in two-terminal quantum ring capacitively coupled to the charged dot was theoretically investigated. The Coulomb interaction between the transferred electron and charged particle confined in the dot, significantly influences the maxima of transmission probability in Aharonov-Bohm effect. When interaction energy is comparable to the lowest excitation energies in the dot then the electron transfers part of its energy to the dot. Thus electron scatters inelastically on the ring which finally leads to a reduction in Aharonov-Bohm blockade and suppression of Aharonov-Bohm oscillation.

ACKNOWLEDGMENTS

We are grateful to B. Szafran for useful discussions. This work was supported by Polish Ministry of Science and Higher Education within the Project No. N N202 103938 (2010–2013). Calculations were performed in ACK–CYFRONET–AGH on the RackServer Zeus.

*chwiej@novell.ftj.agh.edu.pl

[1] Y. Aharonov and D. Bohm, Phys. Rev. **115**, 485 (1959).
[2] R. A. Webb, S. Washburn, C. P. Umbach, and R. B. Laibowitz, Phys. Rev. Lett. **54**, 2696 (1985); G. Timp, A. M. Chang, J. E. Cunningham, T. Y. Chang, P. Mankiewich, R. Behringer, and R. E. Howard, *ibid.* **58**, 2814 (1987); M. Bayer, M. Korkusinski, P. Hawrylak, T. Gutbrod, M. Michel, and A. Forchel, *ibid.* **90**, 186801 (2003); S. Gustavsson, R. Leturcq, M. Studer, T. Ihn, and K. Ensslin, Nano Lett. **8**, 2547 (2008).
[3] A. Fuhrer, T. Ihn, K. Ensslin, W. Wegscheider, and M. Bichler, Phys. Rev. Lett. **91**, 206802 (2003).
[4] W. G. van der Wiel, Yu. V. Nazarov, S. De Franceschi, T. Fujisawa, J. M. Elzerman, E. W. G. M. Huizeling, S. Tarucha, and L. P. Kouwenhoven, Phys. Rev. B **67**, 033307 (2003).
[5] U. F. Keyser, C. Fühner, S. Borck, R. J. Haug, M. Bichler, G. Abstreiter, and W. Wegscheider, Phys. Rev. Lett. **90**, 196601 (2003).
[6] E. Strambini, V. Piazza, G. Biasiol, L. Sorba, and F. Beltram, Phys. Rev. B **79**, 195443 (2009).
[7] R. Leturcq, L. Schmid, K. Ensslin, Y. Meir, D. C. Driscoll, and A. C. Gossard, Phys. Rev. Lett. **95**, 126603 (2005).
[8] M. Sigrist, A. Fuhrer, T. Ihn, K. Ensslin, S. E. Ulloa, W. Wegscheider, and M. Bichler, Phys. Rev. Lett. **93**, 066802 (2004).
[9] A. Yacoby, M. Heiblum, D. Mahalu, and Hadas Shtrikman, Phys. Rev. Lett. **74**, 4047 (1995).
[10] E. Buks, R. Schuster, M. Heiblum, D. Mahalu, and V. Umansky, Nature (London) **391**, 871 (1998).
[11] L. Meier, A. Fuhrer, T. Ihn, K. Ensslin, W. Wegscheider, and M. Bichler, Phys. Rev. B **69**, 241302(R) (2004).
[12] S. Gustavsson, M. Studer, R. Leturcq, T. Ihn, K. Ensslin, D. C. Driscoll, and A. C. Gossard, Phys. Rev. B **78**, 155309 (2008).
[13] A. Fuhrer, S. Lüscher, T. Ihn, T. Heinzel, K. Ensslin, W. Wegscheider, and M. Bichler, Nature (London) **413**, 822 (2001).
[14] T. Ihn, A. Fuhrer, T. Heinzel, K. Ensslin, W. Wegscheider, and M. Bichler, Physica E **16**, 83 (2003).
[15] P. Mohanty, E. M. Q. Jariwala, and R. A. Webb, Phys. Rev. Lett. **78**, 3366 (1997).
[16] A. Mühle, W. Wegscheider, and R. J. Haug, Appl. Phys. Lett. **91**, 133116 (2007).
[17] We made several simulations for wider overlapping parts, i.e., for 200 nm, and did not find any change in results.
[18] T. Chwiej and B. Szafran, Phys. Rev. B **78**, 245306 (2008).
[19] We checked that results obtained for potential step $\Delta V = 0.19$ meV (negatively charged dot) when the range of the Coulomb interaction between particles is limited to 600 nm were identical with those for $\Delta V = 0.28$ meV. It results from the fact that in both cases the same low-energy part of the electron wave packet reflects due to Coulomb interaction and does not enter the ring at all.
[20] B. Szafran and F. M. Peeters, Phys. Rev. B **72**, 165301 (2005).
[21] T. Chwiej and B. Szafran, Phys. Rev. B **79**, 085305 (2009).
[22] A. Chaves, G. A. Farias, F. M. Peeters, and B. Szafran, Phys. Rev. B **80**, 125331 (2009).